

České Vysoké Učení Technické v Praze
Fakulta jaderná a fyzikálně inženýrská

Rešeršní práce

Dentální zobrazování pomocí pixelových detektorů

Vratislav Chudoba

Vedoucí práce: Ing. Carlos Granja, PhD.

Praha 2006

Czech Technical University in Prague
Faculty of Nuclear Sciences and Physical Engineering

Review work

Dental imaging using pixel detectors

Vratislav Chudoba

Supervisor: Carlos Granja, PhD.

Prague 2006

| | | |
|---|--|-----------|
| I. Introduction | | 7 |
| II. Sources | | 8 |
| 1) <u>X-ray tubes</u> | | 8 |
| – <i>device</i> | | 8 |
| – <i>spectrum</i> | | 9 |
| – <i>filtration</i> | | 9 |
| – <i>focal spot</i> | | 9 |
| – <i>exposure time</i> | | 10 |
| 2) <u>Synchrotron</u> | | 10 |
| 3) <u>Other sources</u> | | 10 |
| III. Detector systems | | 11 |
| 1) <u>Criteria and concepts in imaging</u> | | 11 |
| – <i>indirect x direct detection</i> | | 12 |
| – <i>analog x digital</i> | | 12 |
| – <i>counting x integrating techniques</i> | | 12 |
| 2) <u>Film</u> | | 13 |
| 3) <u>Photostimulable Phosphor Detectors (PSP)</u> | | 13 |
| 4) <u>Semiconductor detectors</u> | | 14 |
| – <i>charged couple device (CCD)</i> | | 14 |
| – <i>silicon microstrip detectors</i> | | 15 |
| – <i>flat panel detectors</i> | | 16 |
| – <i>indirect detection flat panel systems</i> | | 17 |
| – <i>direct detection flat panel systems</i> | | 17 |
| – CMOS | | 18 |
| – Hybrid pixel detectors | | 19 |
| – <i>CCD to CMOS hybrid</i> | | 19 |
| – <i>CMOS to CMOS hybrid</i> | | 19 |
| – <i>silicon on insulator (SOI) hybrid</i> | | 20 |
| – <i>Medipix</i> | | 20 |
| IV. System layout and geometry | | 23 |
| 1) <u>Basic phenomenae</u> | | 23 |
| – <i>blurring</i> | | 24 |
| – <i>magnification</i> | | 24 |
| – <i>focal spot in relationship to magnification</i> | | 24 |
| – <i>scattered radiation in projection imaging</i> | | 25 |
| – <i>antiscatter grid</i> | | 25 |

| | |
|---|-----------|
| – <u>slot-scanning geometry</u> | 25 |
| – <i>tube setting</i> | 26 |
| 2) <u>Geometrical modalities</u> | 26 |
| – <i>diagnostic lay-out</i> | 26 |
| – <u>in-line systems</u> | 26 |
| – <u>computed tomography (CT)</u> | 26 |
| – <u>phase imaging</u> | 27 |
| V. Data acquisition and analysis | 28 |
| 1) <u>Analog-to-digital conversion</u> | 28 |
| 2) <u>Intrinsic pixel troubles</u> | 29 |
| – <i>dead pixels</i> | 29 |
| – <i>dark noise</i> | 29 |
| 3) <u>Image reconstruction</u> | 29 |
| 4) <u>Image corrections</u> | 30 |
| – <i>use of convolution</i> | 30 |
| 5) <u>Gray scale</u> | 30 |
| 6) <u>Acquisition time</u> | 31 |
| 7) <u>Subtraction radiography</u> | 31 |
| VI. Conclusion | 32 |
| VII. Acknowledgements | |
| VIII. Apendices | 33 |
| – Appendix A: Image quality | |
| – Appendix B: Biological background | |
| IX. References | 38 |

I. Introduction

Since the discovery of X-rays in 1895, film has been the primary medium for capturing, displaying and storing of radiographic images. However such conventional radiographic techniques for dental imaging purposes exhibit still a number of limitations such as low detection efficiency, poor contrast, narrow dynamic range, limited spatial resolution and require not necessarily negligible doses to patients [1], [2], [3]. On the other hand, with the arrival of electronic and active devices, digital radiography has become a useful tool in dental imaging specially for laboratory and experimental work.

Using newly developed high performance position sensitive semiconductor detectors, modern digital radiographic methods offer a number of advantages such as high detection efficiency, continuous and real-time data acquisition and image generation, off-line image processing and enhancement linear response, wide dynamic range, enhanced contrast and lower radiation doses to patients with satisfactory spatial resolution [1], [2]. The development of suitable imaging systems with these capabilities is desirable and promising in modern dental imaging [1], [2], .

This work focuses on radiographic imaging with high resolution position sensitive digital active detectors [4], [5], [6], [7], [8], [9], [10], [11], [12]. I review the current state of knowledge according to the following sections: sources, detector systems, imaging layout modalities, data acquisition and image reconstruction. I place emphasis on state-of-the-art systems with high spatial resolution, high efficiency and high contrast for digital real-time dental imaging. Citations to scientific papers and publications are included throughout the text including review books [1], [2], [3], MSc. and PhD. thesis [4], [5], [6], [7] and research papers [8-42]. A number of important concepts used to describe and quantify image quality are included in the appendix also with a brief description of the anatomy of teeth and of a dental implant.

II. Sources

Content:

| | |
|--------------------------------|----|
| 4) <u>X-ray tubes</u> | 8 |
| – device | 8 |
| – spectrum | 9 |
| – filtration | 9 |
| – focal spot | 9 |
| – exposure time | 10 |
| 5) <u>Synchrotron</u> | 10 |
| 6) <u>Other sources</u> | 10 |

This chapter reviews the current status of X-ray sources for both routine and laboratory dental roentgenography. The X-ray energy spectrum suitable for dental imaging purposes falls in the range 10 to 50 keV. The conventional standard physical process used for imaging is absorption (i.e., beam attenuation). Thus, X-ray sources are accordingly designed and used.

1) X-ray tubes

The most widespread X-ray source for general dental imaging is the X-ray tube. X-rays are produced, when highly energetic electrons emitted from the cathode and accelerated by an electrostatic potential (of several ten's of kV) fall into the anode where their energy is converted into electromagnetic radiation (bremsstrahlung and characteristic radiation). The efficiency of these processes is relatively small and more than 99% of the incident energy is converted into heat [1], [2].

device

X-rays tubes (shown in Fig. II.1) contain a heated filament (cathode) and an anode made of high-Z materials (such as Thungsten, Rhenium, Molybdenum) [1], [2], [3]. For some applications, modern clinical X-ray tubes contain a rotating anode to dissipate the heat produced. Many tubes have two filaments, a large one and small one, depending on tube output and resolution requirements.

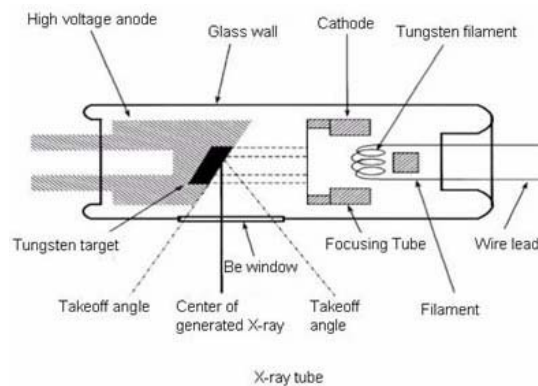


Fig. II.1: X-ray tube layout. Taken from **Chyba!**

II. Sources

The operator can select the tube kilovoltage, tube current and exposure time appropriate for his purpose.

spectrum

Typical dental X-ray tube sources yield currents in the range μA – mA and a continuous broad energy spectrum in the range 10 to 100 keV [1]. The maximum energy of radiation is determined by the voltage between electrodes. For diagnostic imaging, electrons are accelerated by a voltage from 20 to 150 kV¹. Thus, the X-ray energy spectrum ranges from 0 keV to the maximum energy accordingly. Tube current is typically from tens of μA to ten mA.

The X-ray energy spectrum from a typical conventional source can be described as a triangle starting at a lower energy peak at about half of the accelerating voltage and ending at the upper energy limit as illustrated in Fig. II.2. The broad continuous spectrum is superposed by characteristic (K, L, ...) atomic shell lines and depends on target material. The low energy end of X-ray tube sources is 0 keV, but technically the measurable radiation starts only at ~ 10 keV² [1], [13], [15]. For imaging human teeth photon energies range from 20 keV to about 70 keV are applicable for diagnostic purposes. Below 20 keV all X-rays are essentially absorbed and will not contribute to imaging [1].

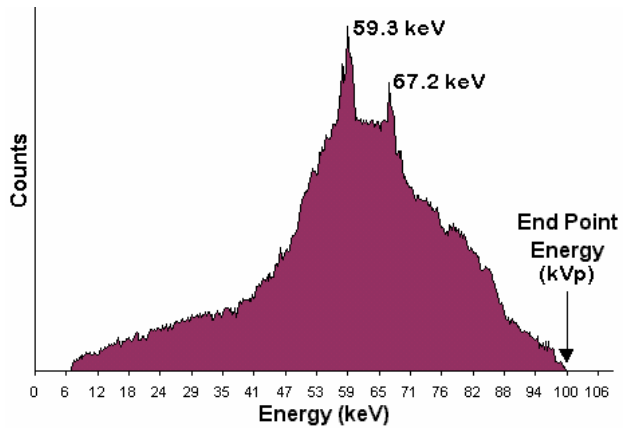


Fig. II.2: Direct tungsten spectrum at 100 kV gained from radiology X-ray machine. Taken from [40].

The broad continuous spectrum is superposed by characteristic (K, L, ...) atomic shell lines and depends on target material. The low energy end of X-ray tube sources is 0 keV, but technically the measurable radiation starts only at ~ 10 keV² [1], [13], [15]. For imaging human teeth photon energies range from 20 keV to about 70 keV are applicable for diagnostic purposes. Below 20 keV all X-rays are essentially absorbed and will not contribute to imaging [1].

filtration

In order to reduce both the dose in the patient and the noise filters are used which cut off bottom part of photon energies.

All X-rays with energies above 60 keV would penetrate a 1 cm thick tooth anyhow and do not enhance contrast, but add noise [13]. The maximum X-ray strength of common X-ray tubes is thus usually set at 30 keV [13] which can be also shifted via filtration to 35 keV [1], [13], [17]. The effect of filtration in the X-ray spectrum is illustrated in Fig. II.3, where energy dependence various filtration materials is plotted.

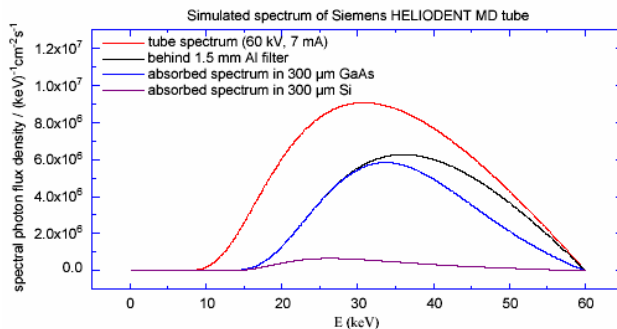


Fig. II.3: Effect of filtration applied on 60 kVp X-ray tube. Taken from [13].

focal spot

For special, high resolution imaging the geometry layout of the imaging setup requires a near point source [1]. In such cases, a small focal spot X-ray tube may be used. The effective focal spot is

¹ Today most of the commercially serially produced dental tubes for routine use allow just two voltage settings: 60 and 70 keV. The first one is used for front teeth and the second one for molars [13].

² Low energy photons (with energy < 10 keV) are readily absorbed by tissue even of few mm thick [3], [2].

considered the width of the beam leaving the source. The influence on image quality is reviewed below in the chapter System layout and geometry.

Today micro-focus X-ray tubes are available with focal spot sizes from 4 to 10 μm ([18], [19], [20]). (Hamamatsu: 5, 8, 10 μm ; Shimadzu: 4 μm , Siemens: 30 μm). A comparison of diagnostic value between microfocus and conventional dental radiographs on the same sample has been done together with the observation of fine bone structures on microradiographs[8], [9], [20].

exposure time

As an important parameter for image quality is the exposure time which is determined namely by the X-ray source intensity and the detection efficiency of the imaging detector device. Typical exposure time settings of the X-ray tubes used for diagnosis are between 0.3 s for a front tooth and 0.8 s for a molar at 60 keV tube voltage [21].

2) Synchrotron X-ray sources

Another type of X-ray source, namely on view to reach beam coherence, high currents and high spatial resolution is to use a much larger and complex device: a synchrotron electron ring accelerator [2].

Synchrotron radiation (SR) is electromagnetic radiation from accelerated charged particles, namely electrons, moving with highly relativistic velocities in storage rings. The SR spectrum extends from the infrared covering visible and ultraviolet light to hard X-rays. The SR intensity in this (X-ray) energy region is several orders of magnitude higher compared with X-ray tubes. Another property of SR is its continuous spectrum without characteristic lines. Therefore, monochromatic radiation with sufficient intensity can be filtered out of the incoming X-rays and the energy of this monochromatic radiation can be readily tuned within an energy range from 5 to 150 keV [22].

The monochromatization of the beam is achieved using a crystal diffraction and/or reflection. Typically, a silicon single crystal set-up is fixed at the source beam exit independent of the beam energy. It is possible to achieve spatial resolution down to several μm [20]. However, with larger sample sizes and for physical reasons, first of all scattering, lead to realistic spatial resolution of 100 μm [22].

This complex expensive radiation source prohibits the use in clinical routine, but for basic research it offers unique possibilities namely in terms of high spatial resolution, intensity and potential to quantification [22].

3) other sources

In addition to X-ray tubes (which are used for common clinical use) and synchrotron electron ring sources (used for specific high-end research studies), the use of radioactive sources remains an open question [23]. Of possible interest may be mentioned beta sources which offer some promising direction of development due to its discrete energy spectrum.

For imaging purposes may be considered beta radioactive sources such as ^{32}P (with maximum energy 1.710 MeV and average energy 695 keV), ^{14}C (with maximum energy of 156 keV and average energy of 49 keV) and ^{35}S (with maximum energy 168 keV and average energy of 49 keV) [23].

However, the low yield and radioactivity (which demands permanent shielding) limit their ultimate use into either clinical or laboratory use.

III. Detector systems:

Content:

| | |
|---|----|
| 1) <u>Basic concepts in X-ray diagnostic imaging</u> | 11 |
| – <i>indirect x direct detection</i> | 12 |
| – <i>analog x digital</i> | 12 |
| – <i>counting x integrating techniques</i> | 12 |
| 2) <u>Film</u> | 13 |
| 3) <u>Imaging plates (PSP)</u> | 13 |
| 4) <u>Semiconductor detectors</u> | 14 |
| – <i>charged couple devices (CCD)</i> | 14 |
| – <i>silicon microstrip detectors</i> | 15 |
| – <i>flat panel detectors</i> | 16 |
| – <i>indirect detection flat panel systems</i> | 17 |
| – <i>direct detection flat panel systems</i> | 17 |
| – CMOS | 18 |
| – Hybrid pixel detectors | 19 |
| – <i>CCD to CMOS hybrid</i> | 19 |
| – <i>CMOS to CMOS hybrid</i> | 19 |
| – <i>silicon on insulator (SOI) hybrid</i> | 20 |
| – <i>Medipix</i> | 20 |

Various general concepts of imaging detector systems are reviewed in this chapter. Single devices are then described in terms of a number of these concepts and additional features such as detector layout, principle of detection, readout scheme, spatial resolution and pixel size, detection efficiency, contrast, dynamic range, exposure time and dose. These criteria are mentioned accordingly and in such sequence, where will be meaningful for a particular detector system. Although this work focuses on digital pixel detectors, the most widely used imaging systems in contemporary practise are reviewed as well, including brief mentions about screen-films and imaging plates. References to currently developed systems are included.

1) Basic concepts in X-ray diagnostic imaging:

Among the most general concepts relevant for X-ray diagnosis imaging may be summarized the following:

indirect x direct detection

In direct photon detection the X-rays are detected and fully converted (absorbed) on the detector material layer itself. All secondary radiation is detected and collected in the same device. Direct detection generally provides better spatial resolution and contrast [1], [2], [19], [22], [24], [25].

In indirect detection use is made of an intermediate layer of sensitive material, which converts X-rays to visible light and only then this visible light is detected in the sensor. Indirect detector systems use a segmented or a bulk scintillation crystal, readout via position-sensitive photodetectors, arrays of photodiodes, or silicon drift detectors [1], [2]. Therefore is the spatial resolution deteriorated, because of lateral spread of the photons which is function of the distance of the light emission point to the detector. In radiology most systems are indirect (screen-film, PSP¹, CCDs²).

analog x digital

In terms of data acquisition and image reconstruction, imaging techniques may be of two types: analog and digital [1], [1][2], [3].

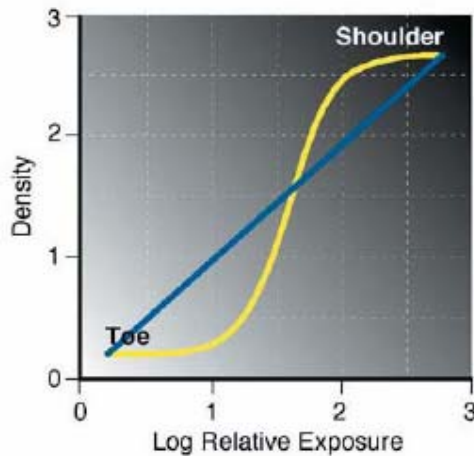


Fig. III.1: Dependence of optical density upon relative exposure for film (yellow) comparison to digital system (blue). Taken from [28].

Most of the images in radiology are still only available on film [1], [2]. The efficiency of film is very low which namely determine exposure times and doses. The image processing of film needs time and expensive materials (film, chemicals).

On the other side, electronic detectors and storage of data in digital form present a number of advantages [1], [2]. Electronic data readout and image reconstruction allow to improve the image quality in terms of contrast, region of interest, sensitivity, sharpness and spatial resolution [4]. For digital detectors is the dependence of optical density upon relative exposure linear. The linearity allows to choose optimally exposure respecting required SNR³ for a specific setup [1] (see a comparison of film and digital system on Fig. III.1). The use of high efficiency semiconductor detectors gives short exposure times and low doses [2].

counting x integrating techniques

Counting and integrating techniques are different approaches how to measure X-ray intensity [1], [2].

In the photon counting method, the signal height from a photon is compared to a threshold set in a comparator. Each photon with energy above the threshold has the same weight of one. The possibility to set a threshold allows, that background noise can be greatly reduced and even eliminated. This feature is associated with improved SNR and dynamic range. Example of single photon counting technique is the state-of-the-art semiconductor detector Medipix [26].

The integrating method does not use a threshold as photons deposit charge in the detector. All incoming signals contain noise and therefore are the SNR and dynamic range reduced [1], [2]. Examples of integrating systems are all screen-films systems, CCDs and imaging plates. Between their advantages belong higher resolution, lower cost compared with counting systems.

¹ Photostimulable Phosphor Detectors

² Charged Couple Devices

³ signal-to-noise ratio, see Appendix A

Among the advantages of photon counting techniques belong: noise suppression, which leads to higher SNR, linear and theoretically unlimited dynamic range and the possibility to cut off Compton scattered photons [1]. Scattered radiation is one cause, why small details and low contrast object are often undetectable. Digital radiographic image detectors are gradually replacing screen-films cassettes.

2) film

These based techniques use X-ray sensitive film to detect and produce images. The film emulsion has an additional layer of silver compound deposited on the film base. The emulsion exhibits poor absorption capability itself and therefore films are practically only used as receptors in screen-films combinations [1]. The intensifying screens absorb part of the X-rays and part of their energy is then re-emitted in form of visible photons which are subsequently detected by the emulsion. The image is captured by emulsion in a latent form and has to be obtained by a separate chemical development process. After development, picture is still fixed only in film and practically cannot be enhanced.

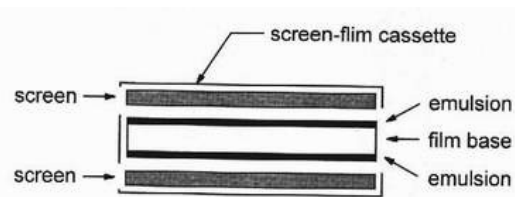


Fig. III.2: Layout solution of screen-film. Taken from [1].

The silver grains are about 1µm large and this dimension exactly determine the intrinsic spatial resolution [22]. Nevertheless, at the photon energy greater than 4 keV the resolution of a microradiography system is determined namely by the range of the photoelectrons in the photographic emulsion. The real spatial resolution of film-based systems is commonly around 20 µm [4]. The usual geometry is dual-emulsion film, where the photoemulsion is placed between two slices of screen to reduce the average light lateral propagation and to improve the spatial resolution (Fig. III.2) [1].

A considerable disadvantage of film systems is their intrinsic integrating and indirect detection mode [1], [2]. Another also significant limitation of film systems is their limited range of exposure. Over- or underexposure result in loss of sensitivity and of contrast. Sheet film has low absorption efficiency for X-rays.

Film based systems still represent the biggest fraction on the market of medical X-ray imaging systems namely for routine work.

3) Imaging plates (PSP)

Photostimulable phosphor detector (PSP) [1], [2], known also as Computed Radiography (CR), storage phosphors or imaging plates belong to indirect detection systems. PSPs are a flexible screen enclosed in a case similar to a screen-film cassette. Plates are typically made of a europium-fluorohalid compounds [1], [2]. When energy is absorbed by imaging plate, part of light is promptly emitted, but much of the absorbed X-ray energy is trapped in the PSP screen and can be read out later. Part of the charge released (electrons) is trapped in a metastable state, where they can remain for days to weeks, with some fading over time. The number of trapped electrons per unit area of the imaging plate is proportional to the intensity of X-rays incident during the exposure [1], [2].

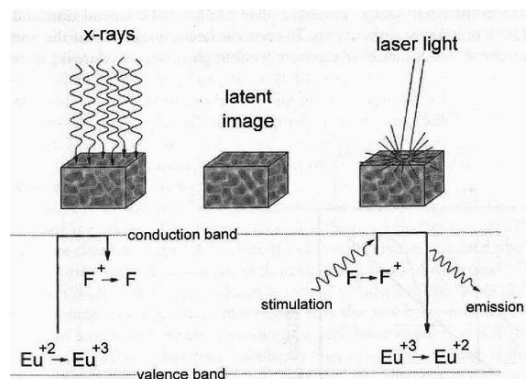


Fig. III.3: Principle of keeping latent image and readout of PSP. Taken from [1].

The imaging plate is exposed in a procedure identical to screen radiography and the cassette is then brought to a PSP reader unit. In this unit the imaging plate is mechanically removed from the

cassette, scanned by a red or near-red laser light (~700 nm), which releases the trapped energy in the form of visible light (mainly between 400 and 550 nm) [1].

When the light scans the exposed imaging plate, the energy of light is transferred to the electron. Electrons gain enough energy to reach the conduction band. These electrons are reabsorbed by europium converting it back to the divalent state (see Fig. III.3). The emitted light is collected by a fiber optic light guide and led to a photomultiplier tube, where is digitised. The readout of the imaging plate does not release all of the trapped electrons and a latent image stays in the plate. To erase the latent image is the plate exposed to a very bright light source, which flushes all of the metastable electrons to their ground state [1], [2].

The PSP have high efficiency and high sensitivity and thus can detect low contrast regions [27]. This feature is related to the sensor's efficiency in detecting X-rays photons, which is also responsible for the decrease in background image noise in dental radiographs.

PSP images present spatial resolution of approximately 6 lp/mm⁴ [28] which is about 100 μm. This resolution is significantly less what can be achieved with conventional film (~20 lp/mm) but not much different from what can be perceived with naked eye (8 – 10 lp/mm) [28]. The limitation is namely due to the spreading out of the stimulating light beam as well as of the released stimulated light, which is a function of the phosphor thickness [2].

Administered doses tend to be slightly higher than for screen-films, but the primary advantages of PSP are their wide and linear dynamic range which make it possible for a greater number of images acceptable for diagnosis [1], [2]. PSP can be used also as a replacement of film cassettes in a conventional X-ray machine setup [27]. Another advantage of the PSP image receptor is that it is cordless. The receptor is flexible and approximately the same size as conventional film.

4) semiconductor detectors

Position sensitive semiconductor detectors present a number of advantages: high efficiency of detection of X-rays (which reduces the exposure time and thus the radiation dose), on-line generation and evaluation of images, high spatial resolution (currently of order of tens μm), energy discrimination and small device size and compact electronics [1], [2], [4], [6], [7].

Charged-coupled devices (CCD)

The Charged-couple device (CCD) is a solid-state detector composed of an array of X-ray or light sensitive pixels on a pure silicon chip [1], [2], [4].



Fig. III.4: Direct digital radiograph of teeth (molars) taken with CCD camera. Taken from **Chyba!**

The principal feature of CCD detectors is that the CCD chip itself is an integrated circuit made of crystalline silicon. A CCD chip has discrete pixel electronics etched onto its surface. There are two types of digital sensors array designs: area and linear [1], [2]. Area arrays are used for intraoral radiography, while linear arrays are used in extraoral imaging. Area arrays are available in sizes comparable to conventional intraoral films, but sensors are rigid and thicker than radiographic film and have a smaller sensitive area for image capture. Area array CCDs have two primary formats: fiberoptically coupled sensors and direct sensors [1]. Fiberoptically coupled sensors utilize a scintillation screen coupled to a CCD, direct sensor CCD arrays capture image directly (see Fig. III.4).

The silicon surface of a CCD chip is photosensitive as visible light falls on each pixel, there are created electron-hole pairs, which are accumulated in potential wells by the electrodes of the CCD. These potential wells are located very close to the surface of the CCD, the pixel array is segmented into a matrix of square potential wells. The number of produced electrons-hole pairs is proportional to

⁴ lp/mm: line pairs per millimeter, this unit is defined in Appendix A

the light intensity falling on each pixel and signals from several events are integrated in the pixel(s) closest to the point of the interaction. A voltage barrier keeps the electrons in each pixel [2].

The CCD requires a significant amount of support electronics, which are not integrated, for operation. High-speed readout is difficult for the CCD because signal charge must be readout in serial fashion [1], [8]. Once the CCD chip has been exposed, the electronic charge that resides in each pixel is read out. Along one column on the CCD chip, the electronic charge is shifted pixel by pixel by appropriate control of voltage levels at the boundaries of each pixel. The charge from each pixel is thus read out one by one, in a shift-and-read process (see Fig. III.5). When the integrated charge of each pixel reaches the output node at the end of the read-out register, it is measured by a charge sensitive amplifier and subsequently digitised by an analog-to-digital converter. Thus as a significant limitation, CCDs have limited dynamic range [27].

A typical CCD pixel is approximately $40\ \mu\text{m}$ size [2]. CCDs with pixel sizes around $10\ \mu\text{m}$ are becoming already available, but spatial resolution is deteriorated mainly by the lateral spread of light photons produced in the convertor layer [8]. Also, pixel cross talk increases dramatically as pixel size is reduced. CCD manufactures minimize charge diffusion by using high-resistivity epitaxial silicon wafers [30]. Acceptable images are possible to obtain with the administration of low radiation dose in CCD-sensors [27].

In contrast to visible light which can be absorbed very well in this thin region, the absorption of X-rays is much less efficient [9]. To increase the absorption efficiency, the CCD may be covered with a scintillator layer [1]. This concept however has the disadvantage of decreasing spatial resolution and contrast due to scattering of conversion photons within the scintillator. In spite of their narrow dynamic range CCDs present acceptable sensitivity at relatively short exposure times and low doses [4].

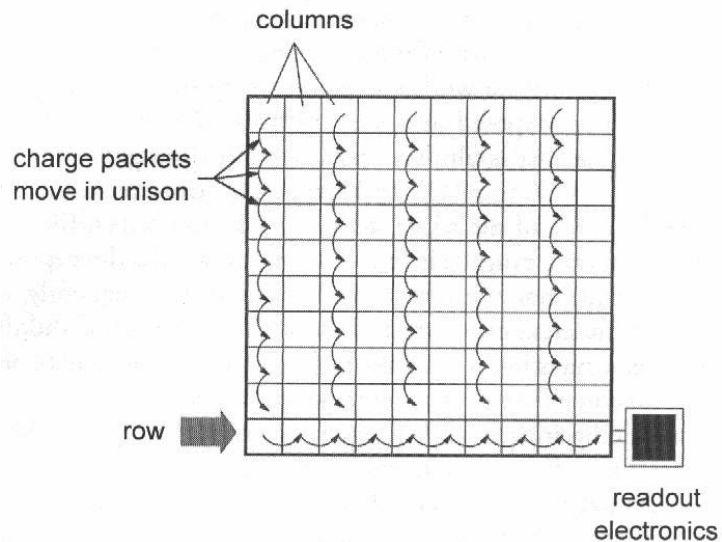


Fig. III.5: Readout scheme of a CCD detector. Taken from [1].

State-of-the-art CCD based systems are available or in development with spatial resolution of over 22 lp/mm and exposure times of about than 80 ms [29].

Silicon microstrip detectors

Although silicon microstrip detectors do not contain real picture elements their whole conception allows to make pixels by data analysis procedure [2], [3], [16]. In this way they may be considered as pixel detectors.

These sensors are based upon a silicon wafer between 100 and 1000 μm thick [16] with applied potential ensuring full depletion. The surface is implanted with a number of thin diodes usually referred to as strips, for charge collection (see Fig. III.6). The strips pitch can be less than $50\ \mu\text{m}$ and 2D position information can be obtained by arranging the strips on opposing faces to be orthogonal. When a photon undergoes interaction and creates charge carriers, the electrons and holes drift under the influence of the electric field to their appropriate strips. The charge is collected by a suitable charge-sensitive amplifier and hence both energy deposited and position can be determined by

analysing the output from all strips on the detector. A spatial resolution of 15 – 20 lp/mm can be achieved [16]. The silicon thickness affects the DQE⁵ of detector. For common thickness of wafers (300 μm) the detection efficiency is about 2,5% for dental applications [16].

X-ray interactions in the silicon wafer deposit energy in the form of charge carriers over a range of distances. This is due to

either electron transport of the photoelectron or to recoil electrons within the material, transport of secondary particles or to Compton scattered photons [3]. The distribution of energy over the detector is due almost entirely to scattered photons depositing energy in neighboring pixels. The range of a scattered photons (10 – 20 keV) in silicon is of the order of a few hundred microns. The charge spreading between pixels can in extreme cases leads to the event that the signal is not detected when the signal is not greater than the pixels noise threshold [16].

This type of detector is still at present in development and seems to be a very promising direction for use in medical imaging. Dental imaging design studies and simulation are underway [16]. Prototype systems using this principle include [2], [16], which present spatial resolution in orders of 15 – 20 lp/mm, low intrinsic noise.

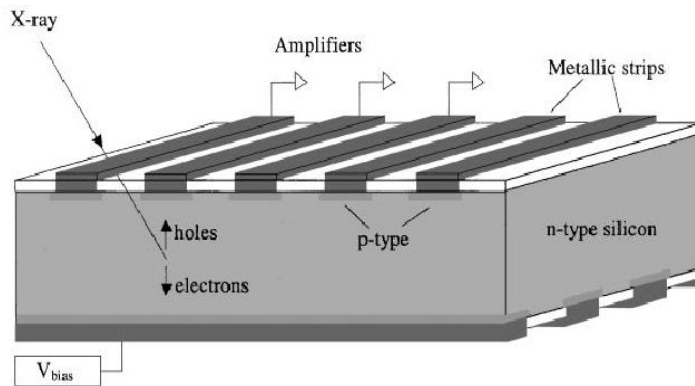


Fig. III.6: Schematic diagram of a double sided microstrip detector. Taken from [16].

Flat Panel Detectors

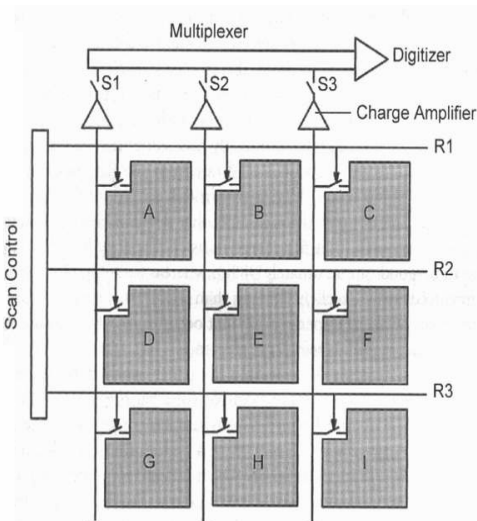


Fig. III.7: Readout process for Flat Panel Detectors arrays. Taken from [1].

Flat panel detector systems consist of a large number of individual detector elements (pixels) working in integrated mode [1], [2], [4]. Instead of producing individual connections to each one of the elements in the system, a series of horizontal and vertical electrical lines are used, which can address each individual element. With this approach only 2000 connections between the imaging plate and readout electronic are required for a 1000x1000 pixel detector, instead a 10⁶ connection [1].

Every individual detector element is capable of storing charge in response to X-ray exposure. Each element has a light-sensitive area and a corner of it contains the readout electronics. Electrons are released in the photoconductor region after exposure to visible light. During exposure, charge is built up in each detector element and is held there by the capacitor. After exposure, the charge is read out by the electronics. During read-out one row after another is activated and the signals are amplified at the end of the column, multiplexed and digitised [1], [2].

⁵ DQE – detection quantum efficiency (see Appendix A)

Each detector element in a flat detector has a field effect transistor (FET) associated with it; the source is the capacitor that stores the charge accumulated during exposure, the drain is connected to the readout vertical line and the gate is connected to the horizontal wire (see Fig. III.7).

The size of the detector element on a flat panel largely determines the spatial resolution. For example, for a flat panel with $125 \times 125 \mu\text{m}$ pixels, the intrinsic maximum spatial frequency is 4 lp/mm, for $100 \times 100 \mu\text{m}$ pixels 5 lp/mm. Since it is desirable to have high spatial resolution, small detector elements are needed [1], [2].

The electronics of each element takes up a certain fixed amount of the area, so for flat detector with smaller detector element a larger fraction of the its area is not sensitive to light and the detection efficiency decreases when making pixels smaller [2], [3]. The ratio of the light-sensitive area to area of the pixel is called fill factor and denotes the detection active area (see Fig. III.8). If a sufficient number of the light photons generated in the intensifying screen are lost due to a low fill factor, then contrast resolution will be degraded [1].

The choice of the detector element dimensions requires a compromise between spatial resolution and contrast resolution. In spite of this, images produced are generally better than those from screen-film systems [4].

The detection process proceeds via direct or indirect mode and are separately described as follows.

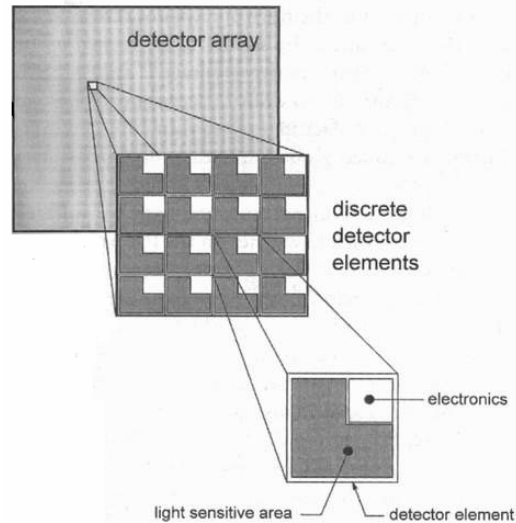


Fig. III.8: A Flat Panel detector contains of large number of pixel, each pixel contains both readout electronic and photosensitive area. Taken from [1].

Indirect detection Flat Panel Systems

Indirect detection Flat Panel Systems make use of an additional conversion layer where an X-ray intensifying screen [4] is used to convert the incident X-ray to visible light.

The large area photodetector consists of a matrix of photodiodes made of hydrogenated amorphous silicon [4]. Flat panels are thicker than film and detect X-rays well. The intensifying screen is layered on the front surface of the flat panel array. Much of the light released in the screen has to travel relatively large distances through this conversion layer which thus leads to some lateral spread of light. To improve this situation, most panels for radiography use CsI screens, which are grown in columnar crystals and act as light pipes to reduce blurring [2].

Current available systems or prototypes of this type of detector systems are underway [1], [2], [4].

Direct detection Flat Panel Systems

The lateral spread of light which decreases the spatial resolution can be minimised by using direct X-ray conversion detectors [1], [2].

Direct flat panel detectors are made from a layer of photoconductor material, commonly amorphous selenium with high stopping ability for X-rays in the diagnostic energy range and homogeneity over large areas [4]. During X-ray exposure, X-ray interactions in the photoconductor material liberate electrons that migrate under the influence of the bias electric field and are collected on the detector elements. The detector is then read out.

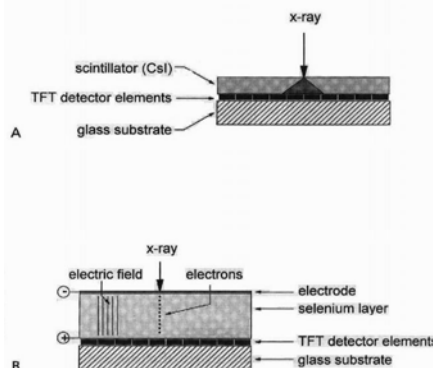


Fig. III.9: The indirect (A) and direct (B) approach on the example of Flat panel detector. Taken from [1].

For direct detection systems electrons are the secondary quanta that carry the signal. Electrons can be made to travel with a high degree of directionality by the application of electric field. Therefore, virtually no blurring occurs in the detector. Furthermore, the electric field can be locally fitted at each detector element by appropriate electrode design, so that the sensitive area of the detector element collects electrons that would otherwise reach insensitive areas of the pixels. This approach increases the effective fill factor [1], [2]. Because of the ability to direct the path of electrons in this type of flat panel, the spatial resolution is typically limited only by the dimensions of the detector element.

One disadvantage is the relatively large amount of energy needed to create an electron-hole pair (~44 eV [4]). For compensation of relatively low X-ray absorption of selenium, these detectors are made much thicker than indirect systems. In order to improve X-ray detection efficiency. For example, a silicon layer of 1,5 mm thickness would be sufficiently efficient in the diagnostic X-ray energy range (1,5 mm Si have an absorption efficiency of ~91% at 70 keV X-ray energy). On the other hand, spatial resolution decreases [4].

Current available systems or prototypes of this type of detector systems are underway [1], [2], [4].

CMOS

Another development of a direct conversion flat panel is the direct conversion in a Complementary Metal Oxide Semiconductor Active Pixel Sensor (CMOS-APS or simply CMOS) [30].

A CMOS pixel chip is either integrated in the sensor material (monolithic approach) or closely connected to the segmented sensor (hybrid approach) and offers a steady increase of amount of functionality and signal processing on the chip [30]. The APS technology reduces by a factor of 100 the system power required to process the image compared with CCD. In addition, the APS system eliminates the need for charge transfer and should improve the reliability and lifespan of the sensor [30].

A special feature of the chip design is the integrated pulse height comparator which discriminates events with charge deposition above the set threshold from those below the threshold including noise signals. An individual photon is either counted as one when the collected charge created in the detector material is above the threshold or else it is ignored [30]. The threshold can be set to correspond to different values of deposited charge. Threshold uniformity over the pixel matrix is improved through the availability of 3 bits per pixel for fine adjustment. CMOS arrays read pixels in a parallel, random access fashion, allowing high-speed operation and low noise performance [30].

Concerning the measurement of the signal charge contained in each pixel, thermal dark-current is relatively high for CMOS arrays. CMOS and CCDs arrays show thermally generated dark spikes or noisy pixels, which create "salt and pepper" in an image (see Fig. III.10). This problem is most pronounced when long exposures are taken and may be solved to certain extent with the use of suitable image software.

Charge collection determines the sensor's ability to reproduce an image. Charge collection efficiency (CCE) is a critical parameter, because it defines the spatial resolution of the detector. Thermal diffusion and weak electric field within a pixel's active volume cause signal electrons to wander into neighboring pixels, creating cross talk and related modulation-transfer function (MTF) loss. Also, pixel cross talk increases dramatically as pixel size is reduced. CMOS arrays show relatively poor CCE performance, because standard foundry processes use low-resistivity silicon wafers. Low-voltage electric operation

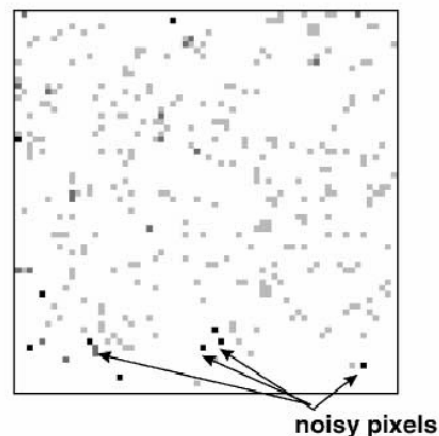


Fig. III.10: Example of flood image taken by detector with noisy pixels. Taken from [33].

(~1,8 V) inherent to CMOS reduces electric field depth. CMOS pixels are directly addressable and are not as sensitive to charge transfer problems as CCDs [30].

Semiconductor materials with a high atomic number (e.g. GaAs) are selected to assure high photon detection efficiency in the photon energy range used in radiology. A 300 μm thick GaAs detector is theoretically ~100% efficient in the detection of photons produced by a dental X-ray tube [21].

An ideal sensor would have 100% quantum efficiency (QE) at all wavelengths. To achieve high response, sensor manufactures must minimize namely three QE loss mechanisms [30]: absorption, reflection and transmission. Absorption loss is associated with optically dead structures. Reflection and transmission losses are inherent to the physical properties of silicon. CMOS arrays experience relatively large absorption loss, because readout electronics incorporated in each pixel are optically dead. Fill factor is usually only between 65 and 75%, compared to a CCD, where the fill factor is 100% [30].

CMOS sensor have thus several advantages including design integration that reduce camera size, low power requirements, manufacturability and low cost, while reliability and lifetime are increasing [30].

However, there are significant limitations associated for single event counting device operated at extremely high count rates required for diagnostic radiology. Factors that influence event rate requirements are image area required, the detection efficiency for the irradiation geometries to be used and the minimum number of events required per pixel to maintain the different aspects of image quality [30].

CMOS sensors have more fixed pattern noise and a smaller active area for image acquisition. A relatively small covering area is the only important issue which has to be solved in the coming years [30]. Nevertheless, state-of-the-art seem promising for intraoral purposes [30].

Current available systems or prototypes of this type of detector systems are underway [1], [4], [27].

Semiconductor hybrid pixel detectors

Another concept is given by hybrid pixel detectors, which consist of a detector and a readout chip which are bonded together by a flip-chip process into a fully integrated hybrid device [2], [4], [5], [6], [11], [12], [16], [26].

A major advantage of this type of hybrid solution compared to monolithic devices like a CCD is the fact, that both chips can be optimised separately [2], [4], [5], [11], [12], [26], [30]. While for the readout circuit the well-known silicon CMOS technology is preferred, materials with enhanced absorption efficiency for X-rays in the energy range 10 – 70 keV such as GaAs or CdTe may be used [21], [26].

Some promising hybrid concepts are reviewed as follows:

CCD to CMOS hybrid

CMOS arrays enable fast signal acquisition through parallel signal processing and integration of CCD pixel and CMOS readout integrated circuit chips into a hybrid array device [2], [30].

The CCD and CMOS chips are joined together with standard indium bump bonds. Backside or frontside illumination is possible [30]. CCD to CMOS hybrid architecture varies significantly [30]. For example a single CCD output port connected to a single CMOS readout chip is employed for slow scan low noise scientific applications. Also, CCD to CMOS technology is susceptible to high-energy radiation damage, a problem also common to CCD monolithic [2], [30].

Current available systems or prototypes of this type of detector systems are underway [1], [2], [4], [30].

CMOS to CMOS hybrid

CMOS to CMOS hybrid is an arrangement, where a backside illuminated CMOS pixel array is bump bonded to a CMOS readout chip [30] as illustrated in Fig. III.11.

Similar to the CCD to CMOS hybrid, the two chips are fabricated independently allowing the CMOS pixel array to be custom fabricated using processes not compatible with the CMOS readout chip. Similar to the CCD to CMOS hybrid, the readout part can be bump bonded to the CMOS pixel array on the sides of the chip. CMOS lithography is limited to fabricating arrays of 20 to 40 mm depending on the manufacturer's alignment capabilities [30]. Unlike CCD type detectors, CMOS pixel arrays read pixels directly without transferring charge from pixel to pixel.

Current available systems or prototypes of this type of detector systems are underway [30], [27].

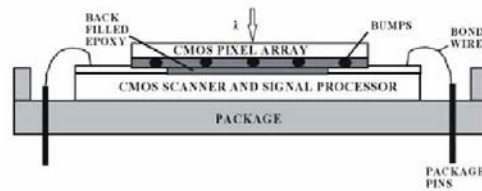


Fig. III.11: CMOS to CMOS hybrid solution (taken from [81])

Silicon on insulator (SOI) hybrid

Development of CMOS imagers fabricated on SOI wafer is still under development. This technology shows high performance compared to conventional bulk technology [30]. SOI wafers include two silicon layers that are separated by an oxide insulator. Current available systems or prototypes of this type of detector systems are underway [30].

Medipix

This new type of hybrid pixel detector was originally developed for high energy physics applications at the European Centre for Nuclear Physics Research CERN [26]. This position sensitive detector is very suitable for detection of low-energy X-rays, especially in the range of medical radiography [2], [4], [5], [6], [7], [10], [11]. In these technology, a photon counting chip system (PCC) which comprises a semiconductor sensor bump-bonded to a CMOS pixel chip serves as the radiation imaging detector. The sensor of the PCC system converts the X-rays directly into electric charge which is collected under the influence of an applied electric field at the pixel electrodes. CMOS pixel size is in order of microns [30].

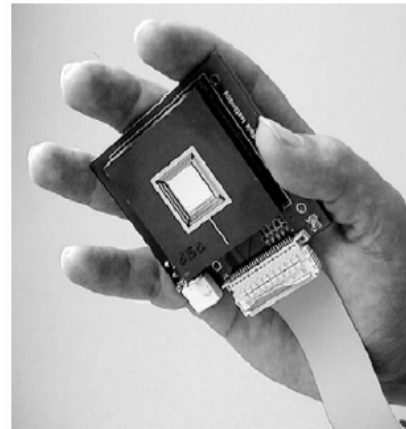


Fig. III.12: A possible solution of Medipix2 detector system for hand-held use, with a cable connection to the readout electronics. Taken from [34].

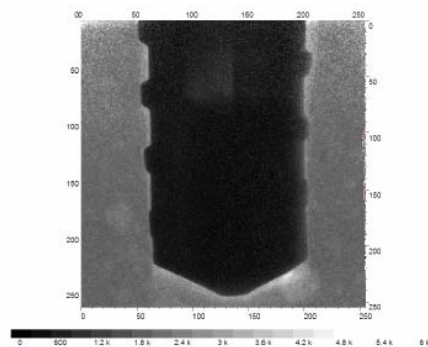


Fig. III.13: Image of implant with layer of wax embedded in plaster acquired with Medipix2. Taken from [81].

The Medipix device is a single photon counting device built in hybrid technology: a conversion material is bump bounded to the electronic readout chip [26], [30]. Contemporary there are two generations of this detector: Medipix1 and Medipix2.

The Medipix1 has 64 x 64 pixels with a pixel size of $170 \times 170 \mu\text{m}^2$, with total active area $\sim 1,18 \text{ cm}^2$ and electronic pixel noise of 2000 e^- [26], [30]. This device was improved into the second generation Medipix2.

The Medipix2 device can have a 300 or 700 μm thick, high resistivity silicon (or also other materials) photon counting detector system with 256 x 256 pixels each of pixel size $55 \times 55 \mu\text{m}^2$ and total active area around 2 cm^2

⁶ electron-hole pairs

representing 87% of entire chip area and low electronic pixel noise of $140 e^-$ [26], [30]. In addition to using different thick active layers, newly is used also CdTe [13] or GaAs [23], [25], [26] as conversion layer for increased detection efficiency.

Each pixel has its own threshold preamplifier, discriminator, with 3-bit individual threshold adjust and digital counter integrated on the readout chip. The counter of a depth of 15 bits assure a wide dynamic range. The individual pixels are connected to the $0,25 \mu\text{m}$ CMOS readout chip via bump bonds [30].

The individual 3-bit adjustments are used for the two discriminators (upper and lower threshold) for each pixel and also the flat field correction to facilitate uniform threshold settings and to smooth out fixed pattern noise. It is thus possible to set an energy window [11], [12], [13], [26].

Up to this day, the Medipix2 readout system is based on a MUROS2 [4], [13], [14] interface with large dimensions and bulky associated electronics devices (power supply, readout PC card). In order to increase the portability and ease of measurement, the current setup has been replaced by a fully integrated new interface based on the USB [5], [11], [12], [26]. The USB-based solution provides both communication and power supplying lines and small dimensions.

The smaller pixel size will lead to an improved MTF⁷, assuming that charge sharing between pixels does not become excessive and thus offer improved detecting quantum efficiency. Thus, doses to patients may be lower by a factor 10 – 100 over current CCDs [15].

Using the energy window enables to significantly improve and enhance thresholds contrast [11], [12], [13]. The relative contrast can be further improved using a narrow X-ray energy window. On Fig. III.14 and Fig. III. 15 is shown how can energy window selection improve and increase contrast. Solution how to smooth a signal noise is in development [30].

In addition to X-ray imaging, the semiconductor Medipix2 detector has been adapted as a digital imaging device for neutron imaging⁸ [9].

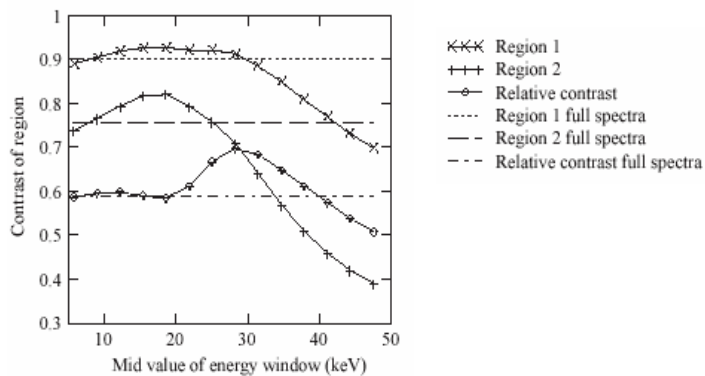


Fig. III.14: Achieved contrast for the two defined regions of tooth (channel and compact crown) and relative between regions for a serie of 4 keV energy windows. Taken from [13].

⁷ Modulation transfer function

⁸ The Medipix2 device with $300 \mu\text{m}$ thick silicon sensor was tested as a neutron detector with different types of converters using neutron beam. Various converter materials were investigated. The neutron converters considered were namely ^6LiF powder, amorphous ^{10}B , cadmium foil and gadolinium. As the best choice appears ^6Li which produced exclusively heavy charged particles and tritons [9]. Secondary heavy charged particles have short range resulting in well localized ionization following with high spatial resolution. There were achieved very promising results in dental neutron imaging, but required devices used as neutron beam (reactors) [9], exclude it from routine dental practise.



Fig. III.15: Images of a tooth (molar) taken by Medipix2 detector using a conventional X-ray tube. Energy window dependent image quality. Window energy are set like 4-8 keV, 26-30 keV and 45-49 keV from left to right. Taken from [13].

For dental roentgenography the system can serve as a high resolution microimaging device with the potential to ultimately provide a tool for in-situ and in-vivo studies of dental implants [8], [9]. The influence of energy selection on improving quality of medical X-rays images was investigated in dental imaging (and also mammography) [6], [7], [8], [9], [13], [25]. Mammography and dental imaging (especially implantology) are in the present days two prime fields which require a perfect imaging properties, like high contrast and spatial resolution [1].

Current available systems or prototypes of this type of detector systems are underway [8], [9], [13], [15], [21], [32], [33], [34].

IV. System layout and geometry

Content:

| | |
|---|----|
| 1) <u>Basic phenomenae</u> | 23 |
| – <i>blurring</i> | 24 |
| – <i>magnification</i> | 24 |
| – <u>focal spot in relationship to magnification</u> | 24 |
| – <i>scattered radiation in projection imaging</i> | 25 |
| – <u>antiscatter grid</u> | 25 |
| – <u>slot-scanning geometry</u> | 25 |
| – <i>tube setting</i> | 26 |
| 2) <u>Geometrical modalities</u> | 26 |
| – <i>diagnostic lay-out</i> | 26 |
| – <u>in-line imaging</u> | 26 |
| – <u>computed tomography (CT)</u> | 26 |
| – <u>phase imaging</u> | 27 |

In this chapter I review the geometry setup and layout of imaging as well as the most common approaches and magnification used to acquire X-ray images in the laboratory.

Regarding the measuring layout, radiography is a transmission imaging procedure [1], [2], where the physical process is absorption. Conceptually different is emission imaging, used in nuclear medicine and diffraction-based phase imaging and reflection imaging [1], [3].

This work is aimed at transmission imaging, which is the most commonly used method.

3) Basic phenomenae

During real imaging acquisitions arise a number of phenomenae, which are directly connected with the geometrical arrangement of the whole imaging system. In this paragraph are reviewed the most important of them.

blurring

Motion is a source of blurring in all imaging modalities. Motion blurring can occur if the patient or the imaging system moves during image acquisition [1]. Blurring occurs through a scattered radiation in matter [2]. It affects image quality and occurs during every real image acquisition. The best way to reduce motion blurring is to reduce the image acquisition time.

The size of X-ray sources, even of microfocus X-ray tubes, have finite size which will always contribute to image blurring. Thus, magnification radiography only works over a selected range of magnification values [1].

magnification

Magnification of the image occurs when the beam diverges from the focal spot to the image plane at increasing distance ratio between source and sample to sample and image plane [1].

The magnification is defined as [1]

$$M = \frac{I}{O}, \tag{IV.1}$$

where I is image size and O object size in the same units. The real source has a finite size, the focal spot. An extended source can be modeled as a large number of point sources. With magnification a geometric blurring occurs in the image Fig. IV.1. The edge blurring f is expressed, in terms of magnification M and focal spot size F [1]

$$f = F(M - 1). \tag{IV.2}$$

There is very readily to see, that blurring depends on the extent of magnification and increases with the size of focal spot and with the amount of the magnification.

focal spot in relationship to magnification

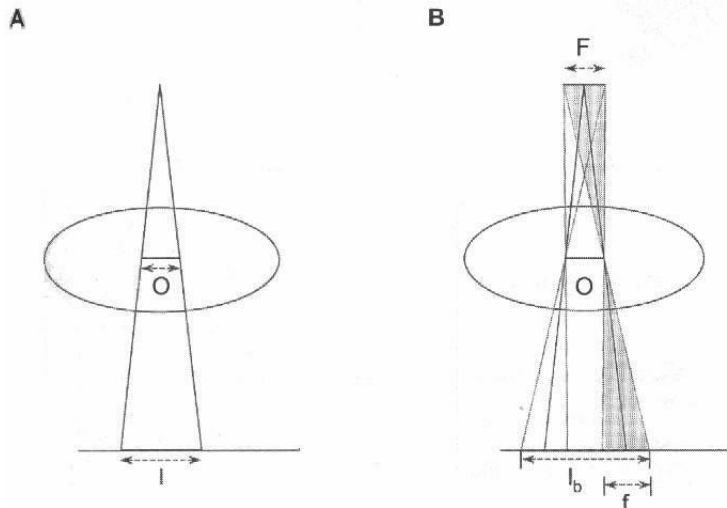


Fig. IV.1: magnification for a point source (A) and for real source with finite focal spot. Taken from [1].

In general-purpose radiographic imaging, relatively large focal spots are used (~0,6 to 1,5 mm), and increased magnification will cause increased blurring of the anatomic detail in the patient. The finite sized focal spot blurs the edges of the objects and reduces their spatial resolution [1].

Nevertheless, if a very small focal spot is used, magnification can be significantly exploited. This is because in some applications, the pixel size limits a spatial resolution (intrinsic spatial resolution of the detector). In

these situations, purposeful magnification can be used with very small focal spots (less than 0,10 mm [2]) to achieve enhanced high spatial resolution [12].

Therefore, microfocus X-ray techniques can be very effective for making detailed observations [11], [12], [24], [19], [20]. Using this approach is possible to distinguish the tissue interface between bone and dental implants at high contrast in high resolution images. Thus, it is feasible for instance to have a non-invasive method to observe and identify the contact between the bone and the implant, the very fine structure of newly formed bone [8], [9], [20] (so called osseointegration [37], [38]).

IV. System layout and geometry

Purposeful magnification radiography is used namely to overcome the spatial resolution limitations of the detector. The limiting factor is namely the decrease in intensity and consequent longer exposure times.

scattered radiation in projection imaging

In addition to the effects above, scattered radiation contributes to the imaging blurring and decreases spatial resolution [1].

Scattered photons disturb the radiographic image, because they do not travel in straight lines between source and detector through the imaged point. This radiation contributes into the detected number of photons, but does not carry (i.e. loses) the information about tissue structure lying directly between the source and the point of detection. The resultant effect is therefore a degradation of the image contrast and SNR.

This image degradation is strongly dependent upon the fraction of scatter to the total number of X-rays detected and has largest effect upon the imaging of low-contrast structures. The contrast C for two region of interest with different attenuation coefficient C_0 , including scattering is determined as [1]

$$C = C_0 \frac{1}{1 + S/P}, \quad (\text{IV.3})$$

where S/P is scatter-to-primary photons ratio and $(1 + S/P)^{-1}$ is the contrast reduction factor. The contribution of scattered radiation at the detector can be significant. For intraoral dental imaging (tissue thickness to 5 cm and detector's size to $5 \times 5 \text{ cm}^2$) are S/P values less than 1 [1].

In tissue, the probability of Compton scattering is about the same as for the photoelectric effect at 26 keV [4]. For materials of higher average atomic number, like bone, the probability for equal contributions of both phenomena occurs at about 35 keV. The scattered radiation incident upon the detector is distributed over angles ranging from 0 to 90 degrees, with a peak between 30 and 40 degrees [2]. Some solutions of this problem are described following.

antiscatter grid

To minimize the scattering effects are used antiscatter grids and air-gaps which are thus used to increase contrast and spatial resolution.. Grids are composed of a series of small slits, aligned with the focal spot, that are separated by highly attenuating dividers. Due to their thickness, usually 3 mm, are grids not used in intraoral imaging [1], [2].

slot-scanning geometry

Another and simple solution is represented by slot-scanning geometry approach [1], [16]. Scatter suppression causes a significant improvement in SNR and contrast [1].

The slot-scanning geometry consists of two slot collimators, each positioned before and after the image object as shown in Fig. IV.3. The X-ray source collimator significantly reduces greater effect on scatter production, and thus reduces patient dose [1].

Scatter is considerably lower the slot-scanning geometry than in the standard geometry.

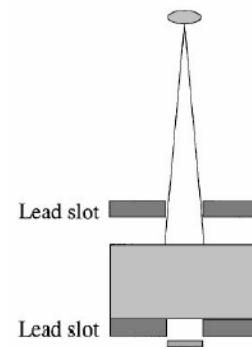


Fig. IV.2: A slot-scanning geometry. Taken from [16].

tube setting

The characteristics of X-ray tubes determine the total exposure time, the radiation dose to the patient and the thickness of the patient participate on the contrast function [1], [2].

Lower kVp result in higher bone versus tissue contrast but also result in substantially higher X-ray doses to the patient [1], [2], [13]. The setting of the device is first of all compromise between contrast and the delivered dose [1].

2) Gometrical modalities

diagnostic lay-out

The common geometrical layout modalities are reviewed [1], [2], namely: in-line imaging, computed tomography and phase imaging [35].

In-line imaging

In the most common radiography arrangement the object is placed between source and detector [1], [2], as illustrated in Fig. IV.3. In intraoral radiography the X-rays are produced in an X-ray tube, which is positioned on one side of the imaged object, pass through the patient and are projected onto the detector at the other side of the patient. Common distances between tooth and tube exit are about 2,5 cm [21]. Sensors are positioned as close as possible to the imaged regions.

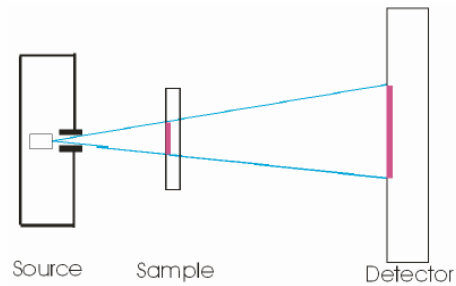


Fig. IV.3: Schematic view on the in-line setup.
Taken from [8].

The gray scale at specific location on the detector is determined by the X-ray attenuation characteristic of the object structure along a straight line through the sample (patient) between the tube and the detector. The source emits a relatively uniform distribution of X-rays towards the patient. After its interaction with the patient's anatomy (namely absorption) the detector records the attenuated (transmitted) X-ray distribution.

Computed tomography (CT)

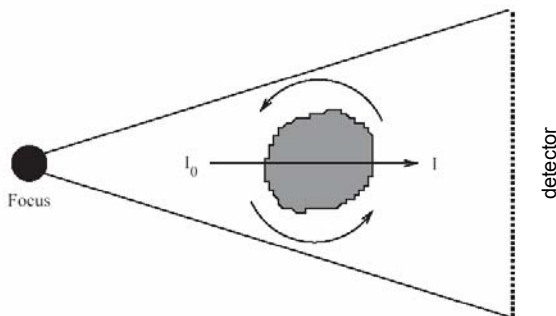


Fig. IV.4: CT geometry with rotating sample. Taken from [32].

As a modification of in-line geometry is computed tomography (CT) [1], [2], [3]. Computed tomography for medical imaging was first introduced by Hounsfield in 1973. In the first systems, this was only possible for a 2D slice of volume elements (voxels). Today a 3D reconstruction is possible with a resolution of about 1 mm in each dimension [1], [2].

There are a number of approaches: In one the X-ray generator and detector are stationary and the sample is rotated on stage (see Fig. IV.4). In another the imaged object is fixed and the source-detector element rotates around it. The first one is mostly used in laboratories for inanimate samples [20] and the second one for conventional clinical use [20]. To obtain a cross-sectional image, the CT scanner system accumulates images at many angles, which serve to reconstruct the inner structural images using a computer algorithms.

Phase Imaging

In addition to particle-like properties, X-rays have also wave-like properties which can be used for imaging [2], [35]. X-ray Phase imaging is fundamentally another method using refraction and/or diffraction of a monoenergetic collimated X-ray beam on transversing the image object [2], [35]. A number of techniques exploit this principle such as X-ray interferometry, Diffraction enhanced imaging and phase-contrast enhanced imaging [35]

Contrary to commonly used X-ray radiology (which is based solely on absorption, i.e., beam attenuation), phase imaging can observe tissue that is otherwise invisible in standard X-ray transmission attenuation techniques. Using this approach information and images can be obtained of low contrast structures and edges while enhancing contrast with high spatial resolution. For instance using a synchrotron accelerator as coherent intense X-ray source, phase enhanced images were obtained from the bone-to-ligament interface and the underlying trabeculae [36]. Using a compact table-top microfocus X-ray source, phase enhanced microroentgenographic images are also possible to obtain thanks to the high performance position sensitive Medipix2 detector [10].

V. Data acquisition and analysis

Content:

| | |
|---|----|
| 1) <u>analog-to-digital conversion</u> | 28 |
| 2) <u>intrinsic pixel troubles</u> | 29 |
| – <i>dead pixels</i> | 29 |
| – <i>dark noise</i> | 29 |
| 3) <u>image reconstruction</u> | 29 |
| 4) <u>image corrections</u> | 30 |
| – <i>use of convolution</i> | 30 |
| 5) <u>gray scale</u> | 30 |
| 6) <u>acquisition time</u> | 31 |
| 7) <u>subtraction radiography</u> | 31 |

In addition to hardware requirements in terms of X-ray sources, detector materials and imaging layout modalities, the data acquisition and image reconstruction techniques are of equal and increasing importance [1], [2], [3]. This chapter is meaningful of course namely to digital systems. In the case of film based systems, the images and information cannot be further processed or enhanced.

analog-to-digital conversion

Digital detectors produce analog data in form of electric charge or current, their readout principles have been discussed above. If such data have to be analyzed by a computer or other digital equipment, they must be converted into digital form. Devices that perform this function are called analog to digital converters (ADCs) and they are an essential component of electronic active detecting and digital imaging systems [3], [4].

Analog signals are continuous in time. However, it is not possible to convert the analog signal to a digital signal at every point in time. Certain points in time must be selected at which the conversion is to be performed, this process is called sampling [1]. Then, each analog sample is converted into a digital signal. An ADC is characterized by its sampling rate (the number of times per second that it can sample) and the number of bits output (the number of bits in the digital number produced each time the ADC samples) [1], [3].

Due to both sampling and quantization, the conversion of an analog signal to digital form causes loss of information. To convert an analog signal to digital form without a significant loss of information content, the ADC must sample of sufficiently high rate [3].

intrinsic pixel imperfections

As digital radiographic detector system have a number of defects and imperfections, a pixel detectors contains some inaccuracies [2]. They originate in process of fabrication, in its principle design itself and its operation.

dead pixels

In pixel detectors there are certain number of detector elements that do not work (they generate no response), so called dead pixels. Fortunately, under most situations these defects and their effect on the image can be corrected using algorithms and data processing.

After manufacture each detector is tested for dead pixels and a dead pixel map is made for each individual detector [33]. Software then use this map for image corrections, where the gray scale values in the pixels surrounding the dead pixel are averaged and this value replaces the gray scale of the dead pixel [2], [3].

Another approach is that the mean pixel counts are not determined by averaging over all pixels, but by fitting a Gaussian to the peak [21]. By this method, the result of the whole array is not falsified by some dead pixels. It was observed, that the distributions were more Gaussian with higher doses. The correction process which removes fixed pattern noise associated with local sensitivity non-uniformity among the pixels improves the SNR significantly [21].

In the care of CCD systems, because of the type of readout architecture systems use, some dead pixels result in the loss of column of data (the charge can not be transfered through the dead pixel). Column defects can also be corrected with the use of interpolation procedures, however, different interpolation techniques are used for column effects than for the dead pixels [1], [8].

dark noise

In the absence of X-rays, each detector element has certain amount of electronic noise associated with it. It is called dark noise and it originates through dark current in the detector and the associated readout electronics [1], [2].

This noise is specific for each detector element and for each exposure. It should be mentioned, that there is virtually no dark noise for the single photon counting systems such Medipix [4], [5], [6], [7], [26]. If there is no exposure, there are no counts in the pixels [4].

This is an advantage compared to integrating devices. Nevertheless, through evaluation of a large number of images obtained by the concrete system, the dark noise can be to some extent averaged and consecutively subtracted from the images [21], [1].

image reconstruction

For practically all detectors, there are slight differences in the sensitivity of each pixel. To correct a differences in gain between the detector elements in the array, a flat field image is acquired. The array is exposed to a homogenous signal and a series of images is acquired and averaged. This operation is realised either directly in a detector or in offline data processing [3].

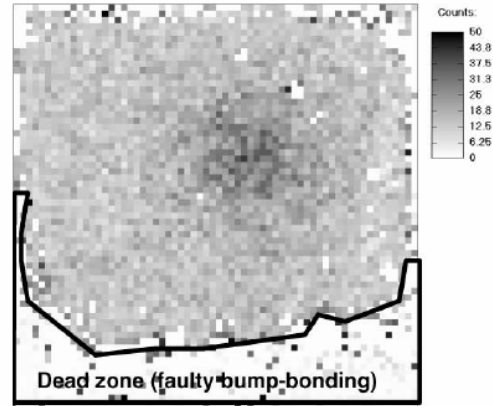


Fig. V.1: Raw image obtained with Medipix1 after 10h of exposure very weak radioactive gamma source. Taken from [33].

For example, a photon counting system can operate with a lower energy threshold set to exclude readout noise. A feature of such system is the ability to adjust the threshold for each individual pixel by defining a calibration mask for the pixel matrix. A calibration mask for the lower threshold can be achieved by software analysis to equalize the noise edge for each pixel [3], [32]. As illustration, the flood image before and after correction is shown in Fig. V.2.

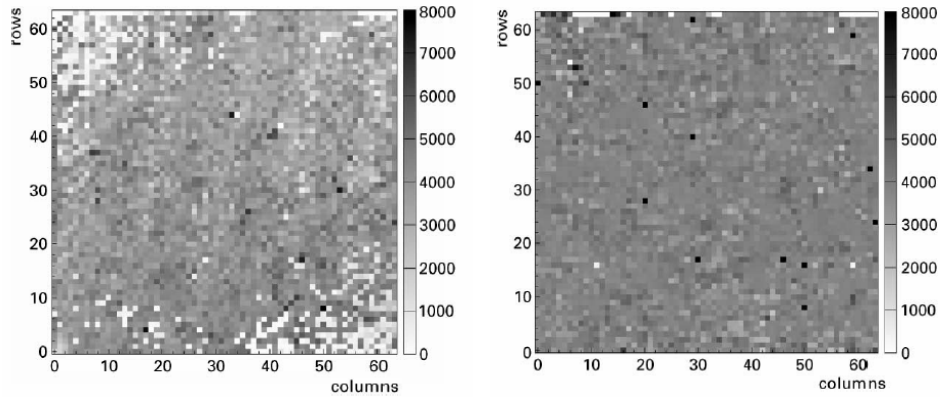


Fig.V.2: Flood image taken with Medipix1 before and after threshold correction. Taken from [21].

image correction

Density and contrast can both be altered off-line after data acquisition using software algorithms [2], [3]. There is a limit to the ability to correct and enhance poor images. Density is manipulated by simply adding or subtracting the same value to each pixel, it means, that it is not possible to save images, in which all pixel have been saturated or where the noise of the system overtop the signal [3].

Convolution

The processing of digital images often makes use of convolution, which is defined mathematically as [1]:

$$g(x) = \int_{-\infty}^{+\infty} I(x')h(x-x')dx', \tag{V.2}$$

where $g(x)$ is the result and $h(x)$ is called the convolution kernel. Using various convolution kernels is possible to improve image quality and enhance contrast and image sensitivity [3].

gray scale

Row of the various levels is called gray scale. Each of this levels is associated with specific optical density [2]. The human eye is able to detect approximately 32 gray levels [28].

It was observed, the better image performance have a systems using a logarithmic gray scale, then these using a linear scale [3]. It lead to the fact, that the

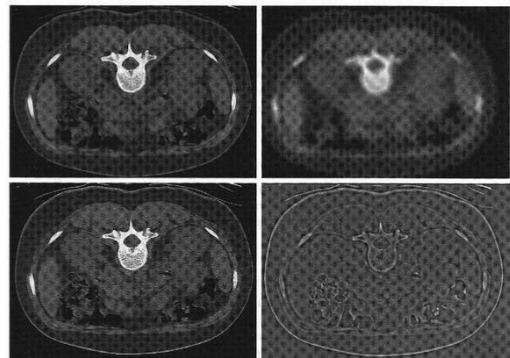


Fig.V.3: Image processed by using a various konvolution kernels. Taken from [1].

professionals take images with a given overall density, using an dose about 40% lower than if linear scale is used [27]. In addition, a logarithmic gray scale visualizes radiographic objects in a way that fits the human eye perception better than a linear scale and is similar to that, which a film radiography provides [27].

Imaging specialists have experimented with pseudocolor image enhancement [28]. While it could seem attractive, the diagnostic utility of this feature has not been demonstrated. The addition of color without understandable gradient provides no new information [3].

acquisition time

The time of image acquisition stands as an important general feature of imaging systems [1], [2], [3]. Generally, for high image quality is required high SNR, which can be obtained by high doses, which are however associated with long exposure times. Is already pointed out, long acquisition time contributes to motion of detector and imaging tissue resulting in blurring. The optimal acquisition time is a compromise between desirable spatial resolution and contrast on one side and level of blurring and dose deposited into a patient on the other side [1], [2].

The relationship between time acquisition is discussed in [21], [32], [1] and [3].

subtraction radiography

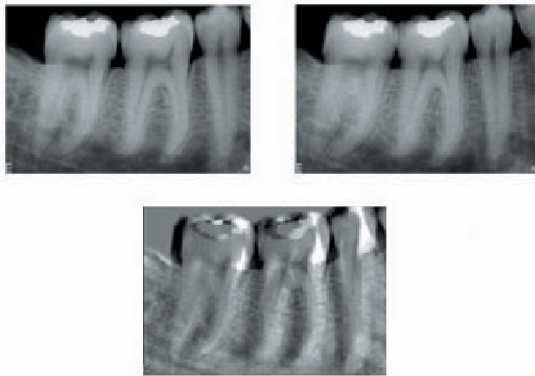


Fig. V.4: Example of use a subtraction radiography.
Taken from [28].

The problem of no quantitative measures to determine the success of treatment is solved using a digital subtraction radiography [28].

It is a technique, that allows to determine quantitative changes in radiograph. An image is generated before a treatment, at some time after treatment another image is generated. These two images are compared on a pixel-by-pixel basis and subtracted those components which are unchanged. The resultant image shows only the changes that occurred (shown on Fig. V.4).

The magnitude of the changes can then be measured by evaluating the histogram of gray levels of the resultant image. This method is associated with a number of setbacks such as system stability and a spatial setting [27].

VI. Conclusions

In this work I made a review of the current state of knowledge of digital radiographic systems for dental medical imaging. I found and reviewed a number of textbooks, MSc. and PhD. thesis as well as scientific papers from conference proceedings and refereed journals concerning digital microoentgenography which are all listed in the References.

The layout of this work was made with view of high performance position sensitive semiconductor detectors which are developed and implemented not only for dental imaging at the Institute of Experimental and Applied Physics of the Czech Technical University in Prague. In terms of this research, it has been verified and compared with other imaging techniques a prototype system using a microfocus source and the high performance position sensitive single photon counting Medipix2 device together with state-of-the-art readout and data acquisition as well as suitable data analysis which as method represents a very promising way for acquiring images. The proposed solution is under development and will include further progress such as improved focal spot size of future next generation sub-micron X-rays microfocus sources, the timepix timing trigger and counting feature and Quad-tiling larger area array of Medipix2 as well as novell unexplored (in the laboratory scale) detection principles such as phase shift contrast enhanced imaging.

VII. Acknowledgements

I would like to thank my supervisor Carlos Granja for suggesting me the topic of this work as well as his advice, guidance and comments.

I would like to thank also Zdenek Vykydal from the IEAP CTU Prague for reading the manuscript and his useful comments.

VIII. Appendices

Content:

| | |
|---|----|
| <u>Appendix A: Image quality</u> | 34 |
| – <i>contrast</i> | 34 |
| – <i>signal-to-noise ratio (SNR)</i> | 35 |
| – <i>detection quantum efficiency (DQE)</i> | 35 |
| – <i>line spread function (LSF)</i> | 35 |
| – <i>spatial frequency</i> | 35 |
| – <i>modulation transfer function</i> | 36 |
| <u>Appendix B: Biological background</u> | 36 |
| – <i>tooth generally</i> | 36 |
| – <i>dental implant</i> | 37 |

Appendix A: Image quality

A number of factors determine the quality of images obtained. Among the most important are the following:

contrast

Contrast is the difference in the image gray scale between closely adjacent regions on the image [1], [3]. The degree of contrast in a medical image is the result of a number of different steps that occur during image acquisition, processing and display. The contrast C of the signal is defined as [1]

$$C = \frac{\Delta I}{I} = \frac{\Delta N}{N}, \quad (\text{VIII.1})$$

where I means intensity of the background signal and ΔI the small difference in intensity compared to this level. For a counting system ΔI can be replaced by ΔN (the difference in the number of counts between the signal and background area) and I by the number N of background counts. Basically C depends on the difference in attenuation coefficients of the viewed detail and the surrounding material, but scattering should be considered as well as it contributes to the measured intensity. The contrast remains unchanged for an increasing number of incident photons (increasing dose), therefore contrast is not the ideal term how to evaluate image quality for radiography.

Signal-to-noise ratio (SNR)

Photonic noise originates due to fluctuations in the number of X-rays absorbed per unit area of the detector. It obeys Poisson distribution with standard deviation \sqrt{N} [1]. Other noise sources are fixed pattern noise, which is related to inhomogenities in the detector and electronic noise from the connected read-out chain. Fixed pattern noise is directly proportional to the signal and can be decreased through a suitable calibration and choice of electronic elements. Electronic noise in integrating systems is proportional to the exposure time [4]. Signal-to-noise ratio (SNR) is defined as [1], [3]

$$SNR = \frac{\Delta N}{\sqrt{N}} = C\sqrt{N} = \frac{\Delta N}{\sigma_N}, \quad (VIII.2)$$

where the terms are the same as for the contrast, σ_N is the standard deviation of the photon count number distribution. A high number of absorbed X-rays improve the SNR and therefore the image quality, but evidently increasing dose. The SNR increases as a function of root square of dose. In all medical X-ray imaging is desirable to reduce the radiation dose to the patient to a minimum level, which means a trade-off between SNR and radiation dose. Common threshold values for the SNR range between 3 and 5 above which a human observer can recognise a detail.

Detective quantum efficiency (DQE)

Real detectors are neither perfect nor ideal and they generally do not absorb (detect) all the X-rays incident upon them. The quantum detection efficiency (QDE) or simply detection efficiency (DE) is the ratio of the number of detected photons to the number of incident photons for a given detector system [1], [3]

$$QDE = \frac{N_{absorbed}}{N_{incident}} = \frac{SNR_{absorbed}^2}{SNR_{incident}^2}. \quad (VIII.3)$$

The DQE for a complex imaging system is the product of the DQE for each stage in imaging chain. Therefore, the DQE for a complete system is never better than the DQE of its weakest component.

Line spread function (LSF)

The LSF describes the response of an imaging system to the line pattern as a measure of the blurring of the image from a very thin line [1], [3]. The broader the LSF the worse is the blurring.

Spatial frequency

Some useful way to express the resolution of an imaging system is to make use of spatial frequency [1], [3]. Use a pattern containing bars and spaces of constant size Δ for one bar respectively space. If an imaging system is capable to differentiate single object, its spatial frequency F is given by relationship

$$F = \frac{1}{2\Delta}. \quad (VIII.4)$$

It is measured in line pairs per millimeter (lp/mm) or cycles per millimeter (cycles/mm).

Modulation transfer function (MTF)

The MTF is the ratio of the amplitude of spatial frequency at the output of the imaging system to the amplitude of the same spatial frequency at the input and describes therefore the ability of the imaging system to reproduce signals of a range of spatial frequencies [1], [3]. The MTF of an imaging system is a very complete description of its resolution properties. The MTF illustrates, how a fraction of an object’s contrast is recorded by the imaging system as a function of the size of the object.

The MTF is preferred LSF as a measure of spatial resolution. MTF can be measured separately for each component of the imaging chain, be superponed and evaluated. The MTF of the system is always lower than the MTF of the worst component. The MTF can be calculated from the LSF using the Fourier transform

$$MTF(f) = F[LSF(x)]. \tag{VIII.5}$$

Appendix B

tooth generally

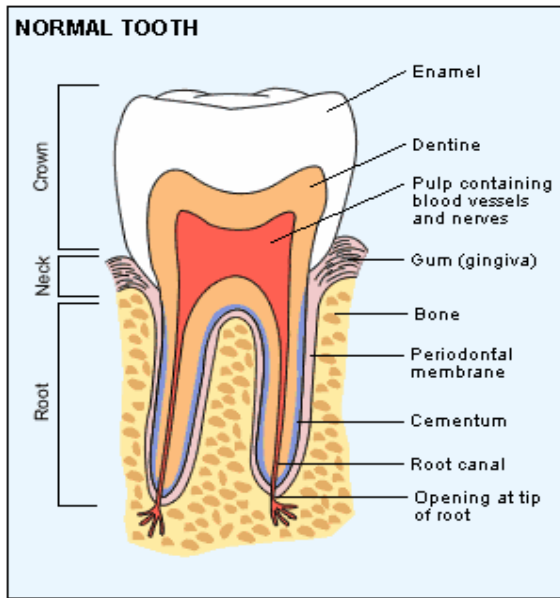


Fig. AppB.1: Schematic illustration of a normal tooth, taken from [39].

In order to make a radiographic images with proper diagnostic value, the anatomy and morphology of human dental region.

Teeth are attached to the underlying bone of the jaw via the periodontal ligament. Jaw is covered with the gum (soft tissue). The white part of the tooth, which is under gum line, is called crown, the region of the teeth at the gum line is the neck and the part below the gum is called root (see Fig. AppB.1). Some teeth have a one root (incisors and canine), all premolars and molars have more root, at most frequently three [39].

The crown is coated by enamel, which is 1 – 3 mm thick and it is the hardest substance in the human body. It is created by tightly packed rows of calcium and phosphorus crystal within a protein matrix structure. Below the enamel is a slightly softer yellow tissue with a structure very similar like bone, called dentin. It contains 45 to 50% of mineral substances, 30%

organic matrix and to 25% of water (volume percentage) [39].

Dentin of root is coated by a thin layer of cementum. Cementum is a hard bone-like substance onto the periodontal membrane attaches. This membrane bound the tooth to the jaw in the bony socket. For cementum and bone decreases a mineral substance ratio on only 45% and vice versa increase the percentage of organic matrix and water, the structure of dentin is not homogenous.

The pulp is the soft tissue in the teeth cavity. This cavity is called the root channel, which generally can has very different shape and spatial and complex structure [39]. The existence of the root channel system is very important for dental diagnosis, because the quality of imaging is judged by the obtained contrast for normal tooth in comparison to the root channel [13]. Dentin is supported by the pulp, which lies in the center of the tooth.

dental implant

As point of this work has been motivated on the view of dental implant imaging [8], [9], a brief review of these objects is include here. Dental implants are surgically fixed substitutes for roots of missing teeth. Embedded in the jawbone, they serve as anchor tooth replacement, or as a full set of replacement teeth [37]. The purpose of dental implant surgery is to fix metallic anchors in the jawbone so, that they can receive the replacement teeth and hold them in place like full-function tooth.

The succes of dental implant is attributed to the osseointegration between the implant material and host bone [20]. For routine cases is time needed to treatment of wound between 6 weeks and 6 months [38], but it is usual to suppose about a few months [36], at most often 3 month [37]. After a period of time, when titanium is succesfully incorporated into bone, direct contact between bone and implant should develop,

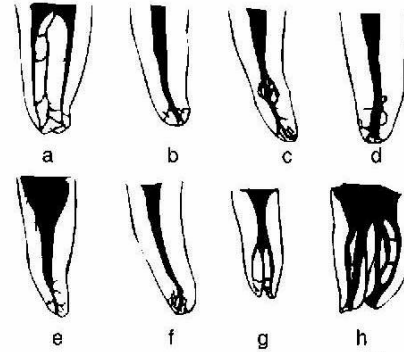


Fig. AppB.2: Complexity of root channel system. Taken from [39].

when osteoblast (cell of bone) grow on and into rough surface of implanted metal. This forms structural and functional connection between a living bone and the imlant. This phenomenon is called osseointegration [38].



Fig. AppB.3: Dental implant taken from the [8].

IX. References

- [1] J. T. Bushberg et al., "The Essential physics of medical imaging", Lippincott Williams & Wilkins, (2002)
- [2] A. Del Guerra, "Ionizing radiation detectors for Medical Imaging", World Scientific (2004)
- [3] C. Guy, D. Ffytche, "Principles of Medical imaging", Imperial College Press (2005)
- [4] B. Mikulec, "Single photon detection with semiconductor pixel arrays for medical imaging applications", PhD thesis, University of Vienna, Austria, (2000)
- [5] Z. Vykydal, "Microprocessor controlled USB interface for Medipix2 detector", Diploma Thesis, Czech Technical University in Prague (2005)
- [6] J. Dammer, "Možnosti použití obrazových detektorů Medipix2 v RTG mamografii", Diploma thesis, Charles University in Prague (2005)
- [7] L. Tlustos, "Performance and limitations of high granularity single photon processing X-ray imaging detectors", PhD thesis, Vienna, CERN – Thesis (2005)
- [8] C. Granja, J. Jakubek et al., "Dental implant imaging with pixel detectors", Proceedings Nuclear Science Imaging Conference IEEE, Rome (2004)
- [9] J. Jakubek, C. Granja, T. Holy et al., "Neutron imaging, tomography and dental imaging with Medipix-2", Proc. Int. Conference on Imaging Technologies in Biomedical Sciences, NIM-A (2006) in print
- [10] J. Jakubek, C. Granja et al., "Phase contrast imaging high resolution X-ray imaging", Proc. First European Conference on Molecular Imaging, Marseille, Nuclear Instrument and Methods – A (2006), in print
- [11] J. Jakubek, D. Vavrik, S. Pospisil et al., "Quality of X-ray transmission radiography based on single photon counting pixel device", NIM A 546 (2005)
- [12] D. Vavrik, T. Holy, J. Jakubek et al., "Experimental setup for high resolution X-ray radiography and tomography", Proc. Nuclear Science Symposium IEEE 2005, October 2005, Puerto Rico, CD-ROM (2005)
- [13] B. Norlin, C. Fröjdh, "Energy dependence in dental imaging with Medipix2", Nucl. Instr. and Meth. A 546 (2005) 19-23
- [14] J. Ludwig et al., "X-ray energy selected imaging with MedipixII", Nucl. Instr. and Meth. A 531 (2004) 209-214
- [15] J. Watt et al., "Dose reductions in dental X-ray imaging using Medipix", Nucl. Instr. and Meth. A 513 (2003) 65-69
- [16] R. D. Speller et al., "Digital X-ray imaging using silicon microstrip detectors: a design study", Nucl. Instr. and Meth. A 457 (2001) 653-664
- [17] C. Hallgreen et al., "The importance of surface texture for bone integration of screw shaped implants: An in vivo study of implants patterned by photolithography", J Biomed Mater Res 57 (2001)
- [18] <http://sales.hamamatsu.com/de/produkte/electron-tube-division/x-ray-products/microfocus-x-ray-source-mfx.php>
- [19] L. Sennerby et al., "A new microtomographic technique for non-invasive evaluation of the bone structure around implants", Clin. Oral Impl. Res. 12 (2001), 91-94
- [20] Kiba H. et al., "Potential application of high-resolution microfocus X-ray techniques for observation of bone structure and bone-implant interface", Int. J. Oral Maxillofac. Implants 18 (2003) 279-285
- [21] C. Schwarz et al., "Dose-dependent X-ray measurements using a 64x64 hybrid GaAs pixel detector with photon counting", Nucl. Instr. and Meth. A 460 (2001) 91-96

VIII. References

- [22] K. Engelke et al., "High spatial resolution imaging of bone mineral using computed microtomography", *Investigative radiology* vol. 28 no. 4 (1993) 341-349
- [23] L. Abate et al., "GaAs pixel arrays for β imaging in medicine and biology", *Nucl. Instr. and Meth. A* 460 (2001) 97-106
- [24] H. Jung et al., "Osseointegration assessment of dental implants using a synchrotron radiation imaging technique: A preliminar study", *Int. J. Oral Maxillofac. Implants* 18 (2003) 121-126
- [25] S. R. Amendolia et al., "Test of a GaAs-based pixel device for digital mammography", *Nucl. Instr. and Meth. A* 460 (2001) 50-54
- [26] <http://www.cern.ch/medipix/> and <http://www.utef.cvut.cz/medipix/>
- [27] S. M. de Almeida et al., "Image quality in digital radiographic systems", *Braz. Dent. J.* 14(2) (2003) 136-141
- [28] E. T. Parks, G. F. Williamson, "Digital radiography: an overview", *J. Contemp. Dent. Pract.* 3(4) (2002) 023-039
- [29] www.dentsply.it
- [30] J. Janesick, "Charged coupled CMOS and hybrid detector arrays", *Focal Plane Arrays for Space Telescope* (2003)
- [31] X. Llopert et al., "Medipix2: a 64-k pixel readout chip with 55- μ m square elements working in single photon counting mode", *IEEE Trans. Nucl. Sci.*, vol. 49, NO. 5, OCTOBER 2002
- [32] Ch. Bert et al., "Computed tomography using the Medipix1 chip", *Nucl. Instr. and Meth. A* 509 (2003) 240-250
- [33] O. Gal et al., "Experimental tests of a hybrid pixellated detector for gamma imaging", *Nucl. Instr. and Meth. A* 460 (2001) 113-118
- [34] K.-F. G. Pfeiffer et al., "Large-scale images taken with the Medipix1 chip", *Nucl. Instr. and Meth. A* 509 (2003) 340-345
- [35] R. Fitzgerald, "Phase-Sensitive X-ray imaging", *Physics Today* – July 2006
- [36] A. Wagner et al., "Qualitative evaluation of titanium implant integration into bone by diffraction enhanced imaging", *Phys. Med. Biol.* 51 (2006) 1313-1324
- [37] <http://www.surgeryencyclopedia.com/Ce-Fi/Dental-Implants.html>
- [38] <http://www.adi.org.uk/public/implant/patientinfo.pdf>
- [39] L. Peřinka, "Základy klinické endodoncie", Quintessenz, Praha (2003)
- [40] <http://www.amptek.com/medical1.gif>